THE AMERICAN SOCIETY OF MECHANICAL ENGINEERS
345 E. 47 St., New York, N.Y. 10017

82-GT-277

Critical Speed in Centrifugal Pumps

S. Gopalakrishnan
Mem. ASME

R. Fehlau

J. Lorett

Technology Department,
Byron Jackson Pump Division,
Borg-Warner Corporation,
City of Commerce, CA

In high pressure centrifugal pumps the magnitude of the critical speed is strongly affected by the presence of liquid in the close clearance spaces of sealing rings and throttle bushings. The stiffening and damping effect resulting from the non-axisymmetric pressure drop across such gaps is often large compared with the elastic stiffness of the shaft. In many cases it raises the critical speed far above the "dry" value, and in some cases it eliminates the critical speed altogether. As a consequence, design specifications based on shaft critical speeds, calculated disregarding the effects of the fluid, become quite meaningless. In this paper simplified equations are derived for the calculation of the effect of the fluid gap. The results have been verified by measurements on a test pump. Sample calculations for a typical multistage boiler feed pump are included as illustration.

NOMENCLATURE

C	damping coefficient
D	bushing diameter
e	eccentricity
F	force
g	acceleration due to gravity
H	nominal radial clearance
K	stiffness
L	bushing length
M,n	mass
N	RPM
n	number of lands
ΔP	pressure drop across bushing
r	radial displacement
W	weight
W_w	equivalent weight of water
ϕ	short circuit factor
λ	friction factor
ρ	fluid density
Θ	angular coordinate
ξ_1	entry-loss coefficient
ξ_2	entry-loss coefficient between groove and land area
ω	angular velocity

SUBSCRIPTS

cr	critical
cr dry	dry critical
cr wet	wet critical
LOM	Lomakin
s	shaft
x	gap
0	reference or nominal condition
1	inlet of bushing
2	just inside bushing
3	outlet of bushing

SUPERSCRIPTS

s	smooth
G	groove
'	narrower part of gap
''	wider part of gap
-	average

Contributed by the Gas Turbine Division of the ASME.

INTRODUCTION

It is well known that an important consideration in the design of the rotating element in a turbomachine is the avoidance of critical speeds. For machines handling air or gases, the prediction of critical speeds is a well-developed technique, and prediction error of under 5% is common. Consequently, the machine designer can confidently avoid the operation of the unit at or near a critical speed. The design specifications for such machines naturally call for adequate separation between the critical speed and the operating speed.

Such design specifications are gradually making their appearance in the pump industry as well. However, the mechanism of critical speed in pumps is much more complex than in gas-handling machinery, and only recently has it become clear that more careful definitions of what is meant by critical speed are necessary.

In particular, it is important to identify two different critical speed concepts for pumps. The first is often called "dry" critical speed or "air" critical speed. This refers to the rotating speed at which vibrations peak if the pump were to operate with no liquid inside it. The second is called "wet" critical speed referring to the normal operation of the pump with liquid in it. Recent research work by the authors has shown that the wet critical speed is vastly different from the dry one, and in some cases, a wet critical speed may not exist at all. Thus it is becoming clear that in most instances, the specification of air critical speed is totally irrelevant.

It is the purpose of this paper to provide the reader with a simplified method for calculating the wet critical speed of pumps. To this end, the paper contains first the theoretical formulation for critical speed calculation. (The necessary mathematical derivation is provided in the Appendices). The calculations are then verified in a suitable test arrangement which consists of a ball-bearing supported rotor with integral wear rings (also called sealing rings). The rotor is driven at a variable speed up to 6000 RPM and vibrations of the shaft are measured near the disk. The pressure difference across the wear rings is controlled independently of the speed by using a separate booster pump. With this arrangement, the pump critical speed can be directly measured by observing the RPM at which vibration amplitudes peak. Various types of wear-ring geometries and clearances were tested and the results are shown in comparison with the calculation. It can be seen that good prediction accuracy is obtained in all the cases. The paper finally concludes with an example calculation for a typical multi-stage boiler feed pump of Byron Jackson design.

THEORY

A liquid surrounding a rotating shaft influences its dynamic behavior in several ways. In low pressure pumps the effect of the virtual mass in close clearances can reduce the critical speed, and the hydrodynamic bearing effect can offer some additional stiffness. In high pressure pumps, however, the strongly predominant effects are those of dynamic stiffness and damping, resulting from the asymmetry of the pressure field of the leakage flow. Both these effects can greatly increase the value of the critical speed over that determined by the mechanical stiffness of the shaft alone.

Numeric expression for these effects are derived in the Appendices, but a simplified explanation in physical terms is as follows:

a) Stiffness.

If a shaft running in a close clearance bushing deflects under the influence of an out-of-balance centrifugal force and assumes an eccentric position in the bushing, the pressure field of the leakage flow along the bushing becomes asymmetrical. This results in a hydraulic force F, resisting the deflection. This force is proportional to the deflection r, and to the pressure drop along the bushing ΔP. The effect can be expressed as a pseudo mechanical stiffness K, where

$$F = - K \cdot r \, \Delta P$$

Since in fluid machines pressures are usually proportional to squares of running speeds, the above expression can be rewritten as

$$F = - \left(K \cdot \frac{\Delta P_o}{\omega_o^2}\right) \cdot r \cdot \omega^2$$

Where ΔP_o is the pressure drop at a nominal speed of ω_o.

In this form it becomes analogous to one describing the centrifugal force caused by a "negative" mass of the magnitude:

$$M_{LOM} = \left(K \cdot \frac{\Delta P_o}{\omega_o^2}\right)$$

This equation is more convenient to use, and the value of M_{LOM} is usually referred to as Lomakin mass, in recognition of the originator of this interpretation of the effect (1).

b) Damping.

The whirling motion of a shaft running in a close clearance bushing gives rise to induced perturbation velocities superimposed upon the velocities of the leakage flow along the bushing. This also causes an asymmetric pressure distribution around the periphery of the bushing and results in forces resisting the whirling motion. These forces are proportional to the velocity of the displacement, and can be expressed as

$$F = - C \cdot \frac{dr}{dt} = - C \cdot r \cdot \omega$$

The value of C is derived in the Appendix. It is, among other things, proportional to the pressure drop along the bushing and its effect can be estimated by comparing it with the magnitude of the critical damping;

$$\xi = \frac{C}{C_{c_r}} = \frac{C}{\sqrt{4 \, K \, M}}$$

Here
C = damping coefficient
C_{cr} = critical damping coefficient
K, M = stiffness and mass of simplified system

c) Effect upon Critical Speed

The effect of the Lomakin mass upon the critical speed can be explained as follows.

Assume a simplified system, comprising a weightless shaft of mechanical stiffness K_S, a concentrated mass m with an initial eccentricity e, and sealing rings and bushings represented by a Lomakin mass M_{LOM}. Running at an angular velocity ω the shaft will deflect under the influence of the centrifugal force by the amount r, determined by the equilibrium of the centrifugal and the restoring forces:

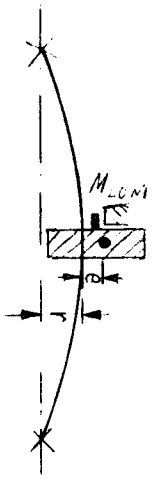

$$m\,(r+e)\,\omega^2 = (K_S + M_{LOM} \cdot \omega^2)\,r$$

This gives the relative deflection as:

$$\frac{r}{e} = \frac{m\,\omega^2}{K_S - (m - M_{LOM})\,\omega^2}$$

Ignoring for the moment the effect of damping and solving for the critical speed, defined by the condition that $\frac{r}{e} \to \infty$, results in

$$\omega^2 = \frac{K_S}{m - M_{LOM}}$$

The same shaft running in air, that is with $M_{LOM} = 0$, would show a critical speed of

$$\omega^2 = \frac{K_S}{m}$$

Evidently, the presence of the Lomakin effect increases the critical speed of the shaft by the factor of:

$$\frac{\omega_{wet}}{\omega_{dry}} = \frac{1}{\sqrt{1 - M_{LOM}/m}}$$

In particular, one should note that if M_{LOM} equals or exceeds m, the critical speed is completely eliminated. This idea can be physically understood as follows: At any given operating speed, the wear ring has a certain stiffness, and this gives a calculable critical speed. If the operating speed is raised to reach this critical speed, the pressure difference across the wear ring will increase, the stiffness will increase, and hence the new calculable critical speed will be higher. Thus increasing the operating speed can keep raising the critical speed such that an actual critical speed can never be reached. Under such circumstances, we can say that a true critical speed is non-existent. It is evident that the condition for such complete suppression of critical speed is simply that the total Lomakin mass of all close-clearance spaces exceed the total mass of the rotating element. This method of appreciating the significance of Lomakin mass was proposed by H. F. Black. (2).

The influence of damping is a further, slight increase in the value of the critical speed, but a much more important effect is that of drastic reduction of deflection when running actually at the critical speed. Expressed in terms of relative deflection the effect of damping is to limit actual deflections at critical speed to the value of:

$$\frac{r}{e} = \frac{1}{2\xi} = \frac{1}{2} \cdot \frac{C_{cr}}{C}$$

Since in most high speed machines the initial eccentricity, e is very small indeed, even a relatively small damping factor of 0.2 limits the critical deflection to approximately 2.5 times the initial eccentricity, a value acceptable in most machines.

TEST ARRANGEMENT

The test pump is a modified Byron Jackson 8 x 10 x 15 DSJH process pump. This is a single stage, double suction, horizontal pump with a ball bearing and a mechanical seal on each end. For the present tests, the impeller was replaced with a solid disk of about the same mass. Wear rings are provided on either side as shown in Figure 1.

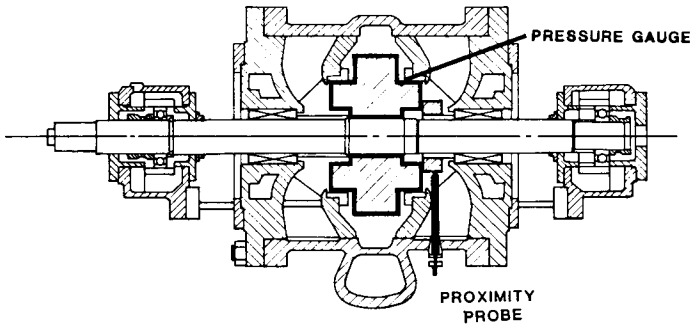

Figure 1. Test Assembly Arrangement

The pump has top suction and top discharge and is driven by a motor powered by a Borg-Warner frequency inverter. The variable speed capability in this set-up was from 0 to about 6500 RPM.

To vary the pressure difference across the wear rings independently of the operating speed, a separate injection pump was used. As shown in Figure 2,

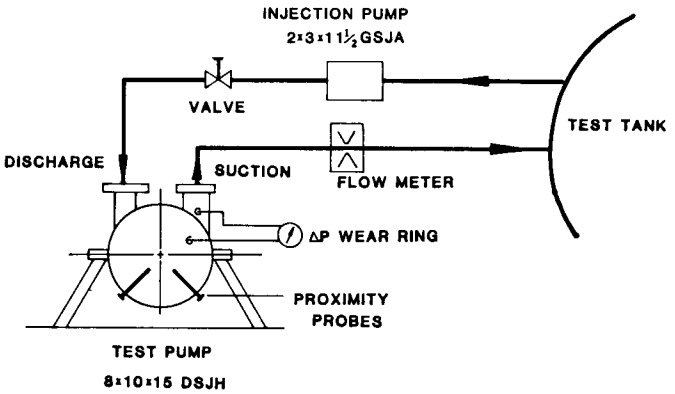

Figure 2. Test Loop

the injection pump is a Byron Jackson 2 x 3 x 11½ GSJA two stage process pump. The output of this pump is

fed to the discharge side of the test pump so that the flow will leak past the two wear rings in the normal direction. This flow then exits the test pump through the suction pipe and returns to the test tank. The pressure difference across the wear rings is controlled by the valve shown in Figure 2, and measured directly. The flow rate is measured using a venturi-type flowmeter.

Shaft vibration amplitudes are measured with two Bently-Nevada proximity probes located close to the disk and circumferentially separated as shown in Figures 1 and 2. The phase shift is measured with respect to a fixed mark on the rotating shaft. The vibration data are reduced to a frequency spectrum at each running speed. All test data shown in this paper are at once/rev. frequency.

TEST RESULTS

1. Tests in Air: The first tests were performed with no water in the test pump and with the wear rings removed. Figure 3 shows the dynamic response

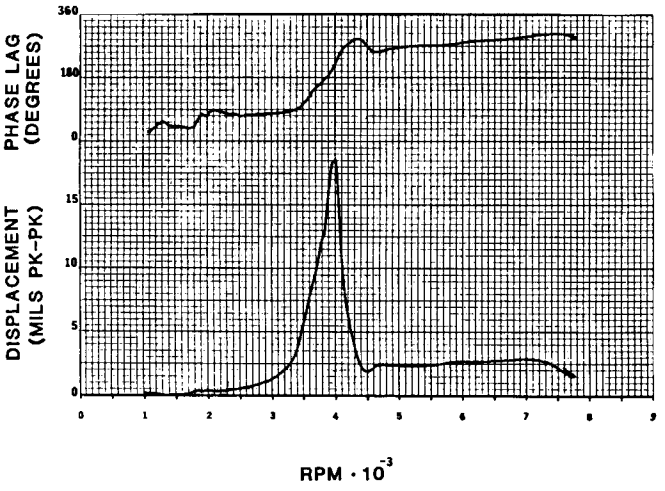

Figure 3. Response in Air

for this case as measured with one of the proximity probes. A clear critical speed at 4000 RPM is observed along with a nearly 180° phase shift.

2. Tests in Water: When water is introduced into the pump, the amplitude response characteristics change dramatically. The response depends strongly on the geometry of the wear rings. The geometrical parameters that were studied are the following:

i) Diametral clearance: Three clearances were tested. .016", .024", and .032"

ii) Grooving Configurations: Tests were made for smooth rings as well as for grooved rings. Effect of grooving only one component (rotor or the stator) and both components were studied separately. Each groove configuration was tested at different clearances.

Figure 4 shows the vibration response for the case of smooth rings with nominal diametral clearance 2H = .016", and pressure difference across wear rings $\Delta P \approx 250$ psi. These are approximately the design point conditions for a pump of this type. No

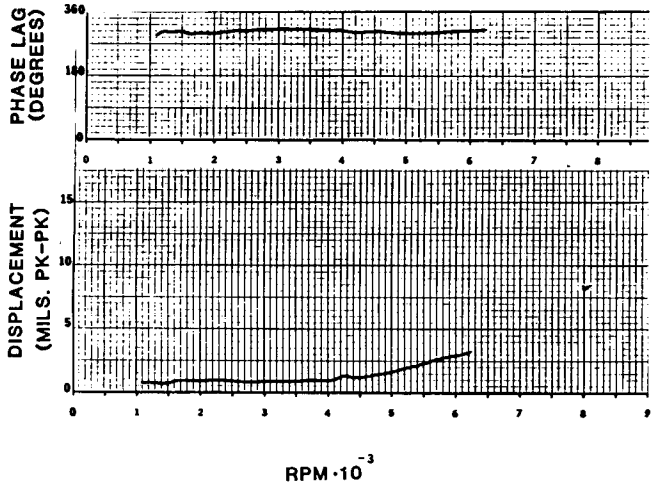

Figure 4. Vibration Response with Smooth Rings and Nominal Diametral Clearance = .016"; ΔP = 250 psi

discernable critical speed is evident within the tested speed range, and there is virtually no phase shift. Figure 5 shows the response for a larger

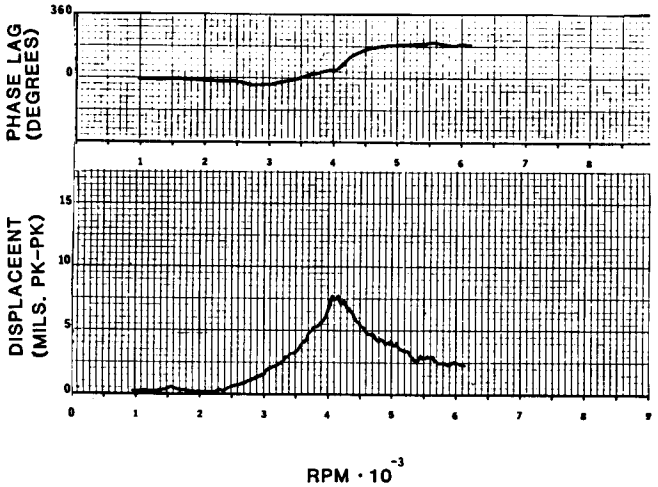

Figure 5. Vibration Response for Smooth Rings with Nominal Diametral Clearance = .032"; $\Delta P \approx 50$ psi

clearance 2H = .032" and $\Delta P \approx 50$ psi. Here the critical speed at 4100 RPM is quite evident and occurs with a 180° phase shift.

Figure 6 shows a typical response curve for the case with both rotor and stator grooved. The groove depth is 3/64", and the land width is 1/16". There are 8 starts, and the grooving direction is to counteract the flow. The clearance 2H = .024", and $\Delta P \approx 250$ psi. The response is harder to interpret, but it is fairly clear that there is a heavily damped critical speed at about 4300 RPM. The phase shift is not 180° but it seems to be on the increase. Such difficulties in interpretation were often encountered with increasing pressures at moderate clearances with the grooving geometry, where the main influence of the liquid film was damping rather than stiffness.

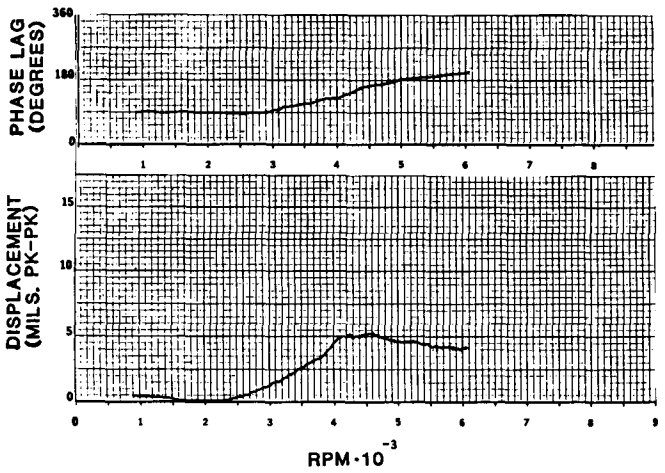

Figure 6. Vibration Response for both Rotor and Stator Grooved Nominal Clearance = .024"; ΔP = 250 psi

COMPARISON WITH CALCULATION

1. Test in Air: The calculation of the critical speed is quite straightforward. The basic dimensions are

Shaft Diameter	2.625"
Bearing Span	34.0"
Impeller Weight	160 lbs
Shaft Weight	60 lbs

From Figure 15.9 of (3) the empirical stiffness coefficient for this configuration is 56, hence

$$K_S = \frac{56 * \frac{\pi}{64} (2.625)^4 * 30 * 10^6}{34^3} = 99600 \text{ lb/in}$$

The combined mass of shaft and impeller is

$$m = \frac{160 + 60}{32.2 * 12} = 0.569 \text{ lb. sec}^2/\text{in}$$

and the critical speed, in RPM, calculates to

$$N_{cr.dry} = \frac{30}{\pi} \sqrt{\frac{K_S}{m}} = 3995 \text{ RPM}$$

This agrees very closely with the measured value of 4000 RPM.

2. Tests in Water: It was noted earlier that the Lomakin effect is usually treated as a virtual mass because its restoring force generally increases as the square of the speed of the pump. In the present test, the pressure across the wear ring is held constant as the test pump speed is increased. Hence the Lomakin effect is independent of speed, and has to be treated as a stiffness. The critical speed is then:

$$N_{cr.wet} = \frac{30}{\pi} \sqrt{\frac{K_S + K_{LOM}}{(W + W_w)} \cdot g}$$

where

W = total weight of impeller and shaft = 220 lbs

W_w = equivalent weight of displaced water = 25 lbs.

K_S = shaft stiffness = 99600 lb/in.

K_{LOM} = Lomakin stiffness at the appropriate pressure drop across the wear ring

g = acceleration due to gravity

For smooth rings, from Appendix 1

$$K^S_{LOM} = \frac{\pi}{4} D \cdot L \frac{\lambda L/2/(1+\xi_1)}{[\lambda L/2/(1+\xi_1) + H]^2} \Delta P \phi$$

With D = 8.5" ; L = 1.625" ; λ = .02 ; ξ_1 = 0.5, we get for two rings:

$$K^S_{LOM} = 20.8 \frac{.0108}{[.0108 + H]^2} \Delta P \text{ lb/in}$$

where H is radial clearance.

Similarly for grooved rings:

$$K^G_{LOM} = \frac{\pi}{4} D L \frac{\frac{\lambda L}{2} (1+\xi_1)}{[\frac{\lambda L}{2} + (1+\xi_1+ n\xi_2)H]^2} \Delta P \phi$$

where n = number of lands

and ξ_2 = entrance loss coefficient between a land and a groove

$$K^G_{LOM} = 20.8 \frac{.0244}{[.01625 + (1.5+11 \xi_2) H]^2} \Delta P \text{ lb/in}$$

The subscripts s and G refer to smooth and grooved configurations respectively. The constant ξ_2 depends upon the groove depth to gap ratio. It can be as low as 0.05 for low values, and up to 0.5 for very large values of this ratio.

Using the above equations, it is a relatively simple matter to calculate the critical speed for all the configurations tested. Figure 7 shows the com-

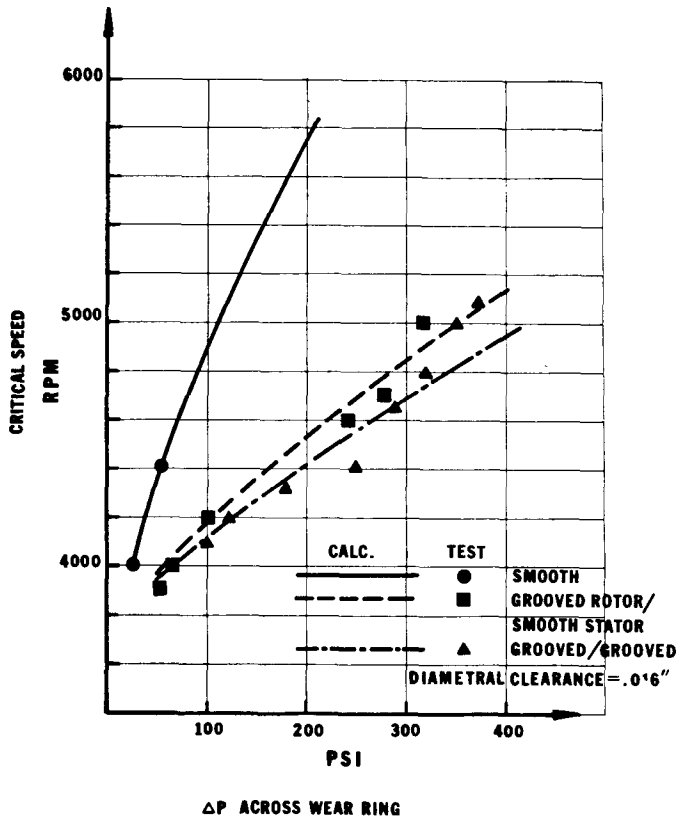

Figure 7. Critical Speed as Function of ΔP across Wear Ring; .016" Clearance

parison for the .016" clearance case. At any given ΔP, the critical speed is highest for the smooth rings. The calculated critical speed agrees very well with the measured values. With one ring grooved, the critical speed is lowered significantly. The calculation tracks this decrease quite well. If both rings are grooved, the critical speed decreases a little bit more, and this trend is also followed by the calculation. It can be seen that, in general, the increase of measured critical speed with pressure is not linear. At high ΔP values, some non-linearities enter into the picture and are not included in the calculations. Figures 8 and 9 show similar results for the .024", and .032" clearance cases. The calculations again provide reasonably good agreement with the measured results.

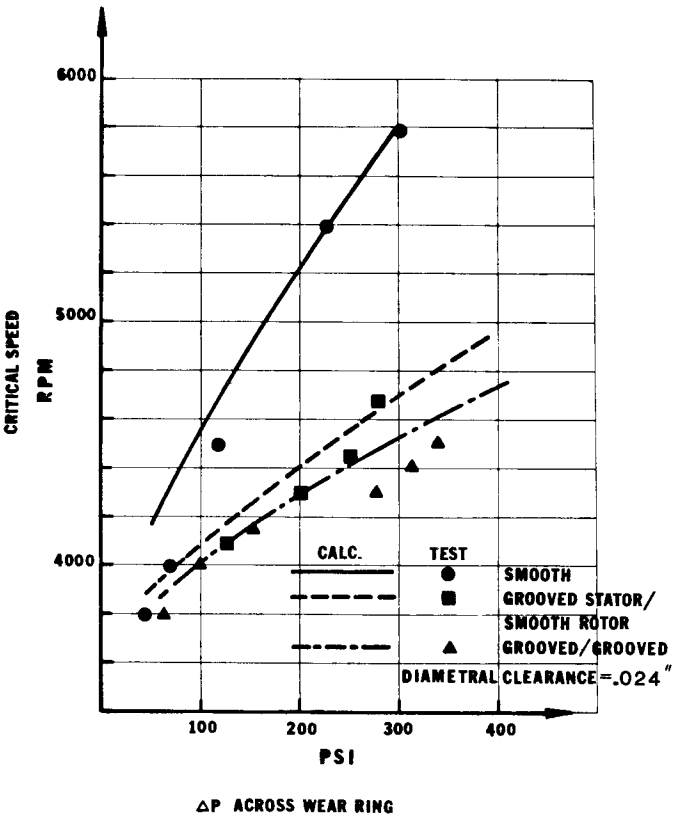

Figure 8. Critical Speed as Function of ΔP across Wear Ring; .024" Clearance

It has sometimes been pointed out that the Lomakin effect rapidly decreases when the ring clearances open up to wear in operation (4). To verify the truth of this statement, the calculated results of Figures 7, 8, and 9 are replotted in Figure 10 showing the variation of critical speed with the clearance. The critical speed with smooth rings can be seen to fall rather rapidly when the clearance is opened up. The decrease is much less rapid for the grooved case. These results are remarkably similar to Figure 6 of (4). However, we find that the rate of decrease is significantly lower than indicated in (4). For example, even if the clearance is opened to 300% of normal value, the critical speed falls only to about 70% of the nominal clearance value. However, since the pump geometries in (4) may be different, direct comparisons can be misleading.

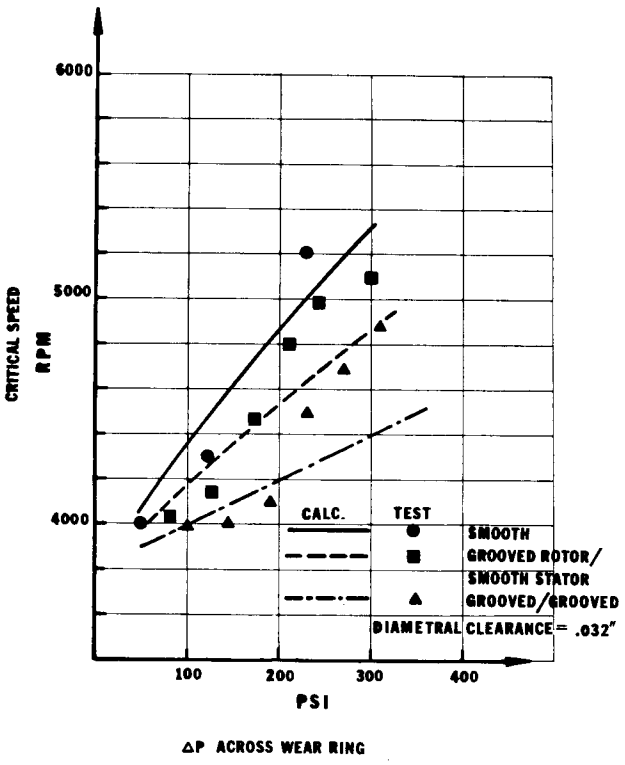

Figure 9. Critical Speed as Function of ΔP across Wear Ring; .032" Clearance

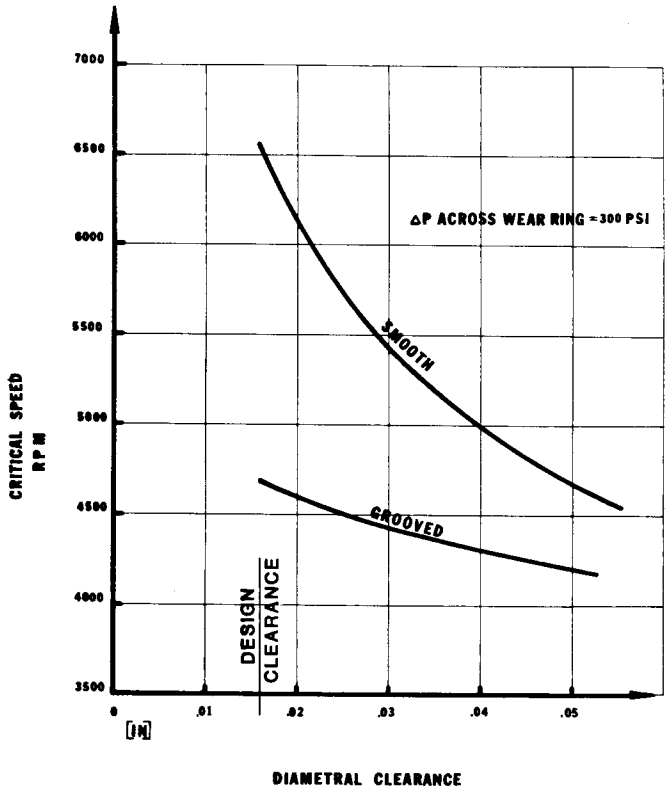

Figure 10. Effect of Wear on Calculated Critical Speed

EXAMPLE CALCULATION

In this section, the wet critical speed is calculated for a 12 x 12 x 14 HSB boiler feed pump containing six stages. The total weight of shaft and impeller is 870 lbs. The important close-clearance spaces are: 6 eye wear rings, 4 hub wear rings, one center-stage piece, and one balance bushing-sleeve. The pressure drop across each ring is carefully determined by allowing for disk friction effects etc. The eye wear rings are smooth, and using the equation in Appendix 1, their equivalent Lomakin weight is calculated to be 6 * 69 = 414 lbs. The hub wear rings are also smooth and their Lomakin weight turns out to be 4 * 53 = 212 lbs. The center stage piece is grooved, but the pressure difference across it is large, i.e., half of the total pump differential pressure. This gives rise to a significant Lomakin weight of 200 lbs. The balance piece is also grooved, and has the same pressure difference. Its Lomakin weight is 195 lbs. If we add up all the Lomakin weights, we find the total to be 1021 lbs, which is well in excess of the shaft plus impeller weight of 870 lbs. Thus the critical speed will be non-existent for this case.

CONCLUSIONS

1) The Lomakin effect in the close-clearance spaces of pumps has a very strong influence on the critical speeds. The effect with smooth rings is much stronger than with grooved rings. In special cases, it is possible for the Lomakin effect to be so strong that critical speed becomes non-existent.

2) The Lomakin effect decreases as the clearance opens up due to wear. Thus the pump critical speed can decrease after many hours of operation. This decrease can be calculated and suitable allowance made at the design stage.

3) A simplified method for calculation of the wet critical speed of pumps is proposed. This method has shown good accuracy against test values for a single stage pump.

ACKNOWLEDGEMENTS

The authors wish to express their deep gratitude to Mr. Ken Templin of Byron Jackson for the initial motivation of this work and also for his continued encouragement and support. The authors also wish to thank Mr. Pat Gonzales, Supervisor of Byron Jackson Dynamics Laboratory, and Mr. Angel Martinez, Supervisor of Pump Development Laboratory, for the acquisition of all test data reported in this paper. Finally, the authors are grateful to the Byron Jackson Management for permission to present this paper.

REFERENCES

1. Lomakin, A.A.; "Calculation of Critical Speed and Securing of Dynamic Stability of Hydraulic High Pressure Pumps with Reference to Forces Arising in Seal Gaps" - Energomashinostroenie Vol 4, No. 1, 1958, pp. 1158.

2. Black, H.F.; "Effects of Fluid Filled Clearance Spaces on Centrifugal Pump and Submerged Motor Vibrations" - Proceedings of the 8th Turbomachinery Symposium, Texas A & M University, 1979.

3. Stepanoff, A.J.; "Centrifugal and Axial Flow Pumps" 2nd Edition, John Wiley & Sons, New York.

4. Makay, E.; "How close are your feed pumps to instability-caused disaster?" Power, Dec. 1980.

APPENDIX 1

DERIVATION OF LOMAKIN MASS

The close clearance geometries that are of interest in the pump industry are the wear rings, center stage pieces and balance bushing sleeves. In order to develop quantitative expressions for the Lomakin mass in such geometries, a simplified model of these rings is made as shown in Figure 11. It indicates a shaft of diameter D located inside an outer stationary ring with a nominal radial clearance given by H. As the shaft executes whirling motion, it is assumed that the shaft center moves in a centered circular orbit of radius e. At any instant of time, the maximum and minimum clearances of H + e and H - e will be established around the periphery. This produces an asymmetry in the pressure distribution around the periphery. The resultant effect of such a pressure distribution is to produce a radial force which will be proportional to the eccentricity of the shaft center.

The pressure distribution along a smooth, narrow sealing gap is characterized by an entry pressure drop, representing the velocity head and an entry loss, followed by a linear pressure drop caused by fluid friction along the flow path. The entry pressure drop can be expressed as

$$\frac{\rho}{2g} V^2 \quad (1+\xi_1)$$

where V = velocity in the gap
ξ_1 = entry loss coefficient
ρ = density of fluid

The friction loss can be expressed as:

$$\frac{\rho}{2g} V^2 \lambda \frac{L}{2H}$$

where
λ = friction ceofficient
H = nominal radial clearance

It is assumed that there will be no pressure recovery at the discharge end.

If a shaft, running in a sealing ring with a radial clearance H, is displaced from the concentric position by the amount e, the gap will vary around the periphery from a maximum of (H+e) to a minimum of (H-e). The overall pressure drop ($P_1 - P_3$), determined by the performance of the pump, will remain the same around the periphery, but the ratio of the friction to the total pressure drop will vary with the size of the gap. Referring to Figure 11, in the

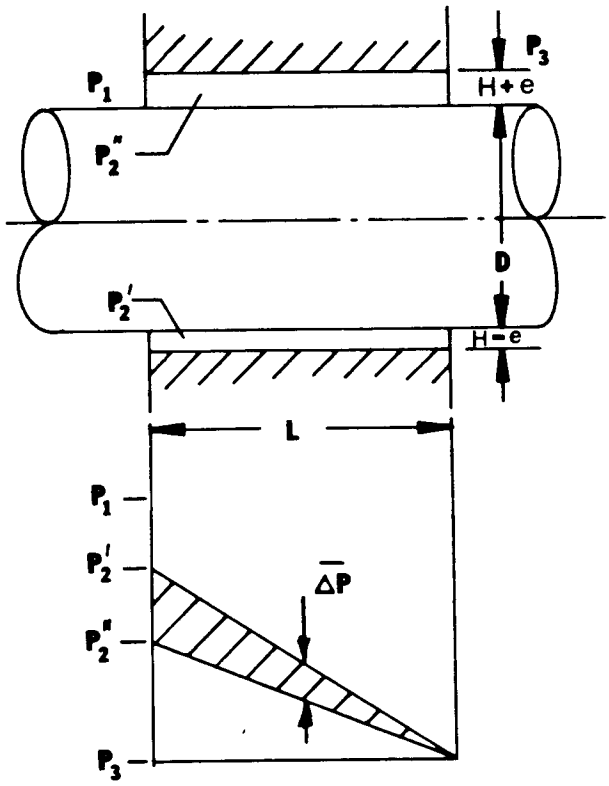

Figure 11. Derivation of Lomakin Mass for Smooth Rings

narrowest spot it will be:

$$\frac{P_2' - P_3}{P_1 - P_3} = \frac{\lambda L/2\ (H-e)}{(1+\xi_1) + \lambda L/2(H-e)}$$

$$= \frac{\lambda L/2(1+\xi_1)}{(\lambda L/2(1+\xi_1) + H) - e} \qquad (1)$$

and in the widest

$$\frac{P_2'' - P_3}{P_1 - P_3} = \frac{\lambda L/2(H+e)}{(1+\xi_1) + \lambda L/2(H+e)}$$

$$= \frac{\lambda L/2(1+\xi_1)}{(\lambda L/2(1+\xi_1) + H) + e} \qquad (2)$$

From Figure 11 it can be seen that the asymmetry of the pressure pattern will cause a mean pressure difference acting upon the shaft of

$$\bar{\Delta p} = \frac{1}{2}\ (P_2' - P_2'') \qquad (3)$$

Defining $\Delta P = (P_1 - P_3)$, and using (1), (2), and (3), we can get:

$$\bar{\Delta p} = \frac{1}{2}\ \Delta P\ \left[\frac{\lambda L/2(1+\xi_1)}{(\lambda L/2(1+\xi_1) + H) - e} - \frac{\lambda L/2(1+\xi_1)}{(\lambda L/2(1+\xi_1) + H) + e}\right]$$

For small deflections, i.e., $e \ll H$, the common denominator simplifies to:

$$(\lambda L/2(1+\xi_1) + H)^2$$

and the pressure difference between the smallest and the widest gap becomes:

$$\bar{\Delta p} = \Delta P\ \frac{\lambda L/2(1+\xi_1)}{(\lambda L/2(1+\xi_1) + H)^2} * e \qquad (4)$$

Integration of the pressure difference around the periphery of the ring results in a restoring force:

$$F = -L \int_0^{2\pi} \frac{\Delta P}{2} \cos^2 \Theta\ \frac{D}{2}\ d\Theta = -\frac{\pi}{4}\ DL\bar{\Delta P}$$

where the negative sign implies a force resisting the displacement. Assuming that the pressure difference generated by the pump follows a square law:

$$\Delta P = \Delta P_o\ \ (\omega/\omega_o)^2$$

the restoring force can be expressed by:

$$F = -\frac{\pi}{4}\ D\ L\ \frac{\lambda L/2(1+\xi_1)}{(\lambda L/2(1+\xi_1) + H)^2} \cdot \left(\frac{\Delta P}{\omega^2}\right)_o * e * \omega^2 \qquad (5)$$

and collecting all constants into

$$M^s_{LOM} = \frac{\pi}{4}\ D\ L\ \frac{\lambda L/2(1+\xi_1)}{(\lambda L/2(1+\xi_1) + H)^2} \cdot \frac{\Delta P_o}{\omega_o^2} \qquad (6)$$

equation (5) can be written as:

$$F = -M_{LOM} \cdot e \cdot \omega^2$$

which is analgous to a centrifugal force exerted by a negative mass equal in magnitude to M_{LOM}. Consequently, the dynamic behavior of the shaft running in close clearance bushings can be calculated by replacing the variable stiffness effects of the bushings by the imaginary negative mass M_{LOM}.

The expression is quite accurate for short rings. In long bushings the circumferential flow tends to reduce the Lomakin effect. The influence can be expressed by a short circuit factor:

$$\phi = \frac{1}{1 + \left(\frac{L}{D}\right)^2} \qquad (7)$$

The Lomakin effect is also present in grooved rings, but is usually less significant. It's magnitude can be derived as follows:

Figure 12 shows a typical configuration. The entry pressure drop can be again expressed as

$$\frac{\rho}{2g}\ V^2\ (1+\xi_1)$$

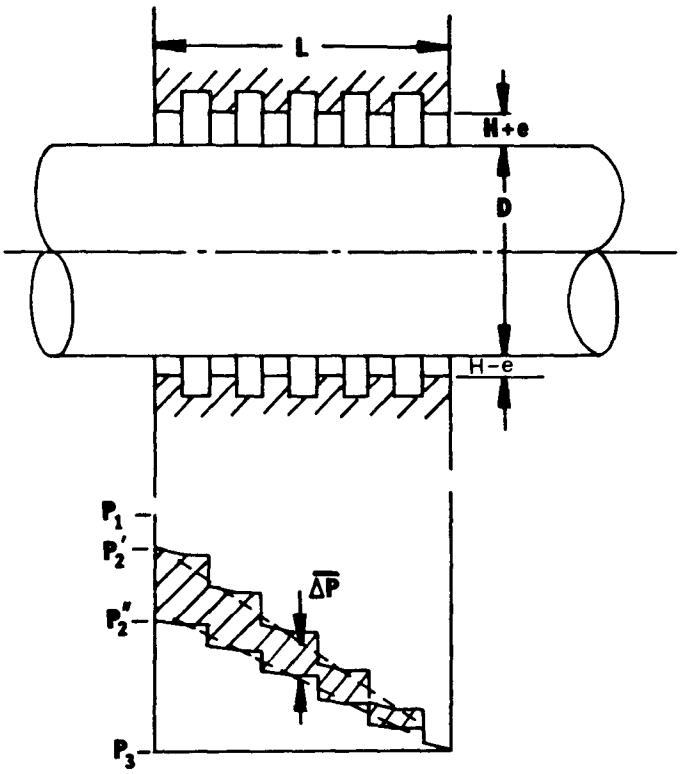

Figure 12. Derivation of Lomakin Mass for Grooved Rings

but the pressure drop along the flow path now consists of the friction loss and of multiple re-entry losses

$$\frac{\rho}{2g} V^2 (\lambda L/2H + n \cdot \xi_2)$$

where n is the number of lands.

Algebraic manipulation, similar to that leading from (1) to (4) gives the mean pressure difference between the narrowest and the widest side

$$\bar{\Delta p} = \Delta P \frac{(\lambda L/2)(1+\xi_1)}{(\lambda L/2+(1+\xi_1 + n\cdot\xi_2) H)^2} \cdot e$$

and further transformation results in the following expression for the Lomakin mass in grooved bushings:

$$M^G_{LOM} = \frac{\pi}{4} D L \frac{(\lambda L/2)(1+\xi_1)}{(\lambda L/2 + (1+\xi_1+ n \cdot \xi_2)H)^2} \frac{\Delta P_o}{\omega^2_o} \quad (8)$$

The value of ξ_2 depends strongly upon the geometry of the grooves, and influences the magnitude of M_{LOM} accordingly.

APPENDIX 2

FLUID DAMPING IN SEALING RINGS (Figure 13)

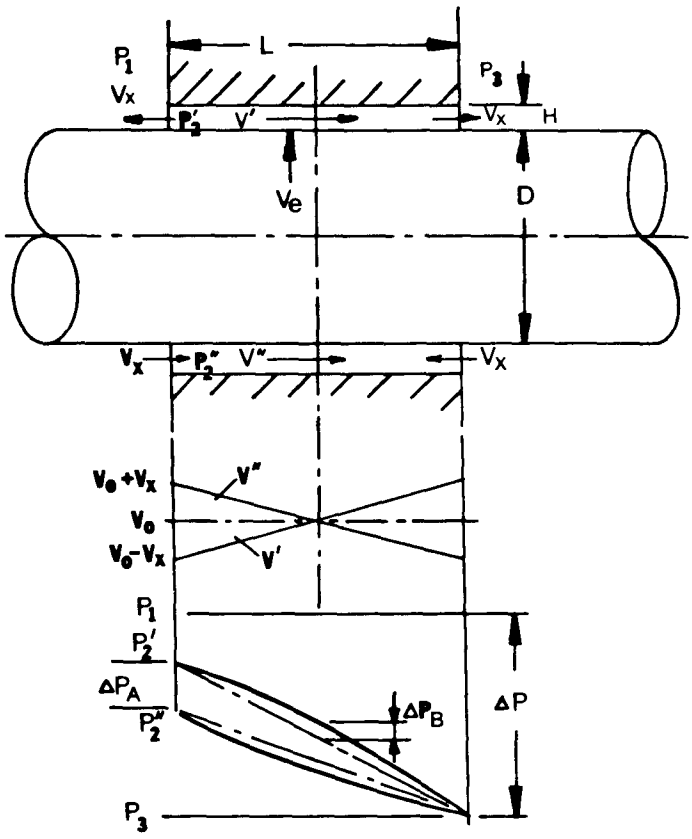

Figure 13. Derivation of Damping for Smooth Rings

The Lomakin effect, described in Appendix 1, resulted in a restoring force in phase with and proportional to the displacement of the shaft. The fluid damping also results in a force resisting the motion, but acting out of phase with the displacement, and proportional to the velocity of the displacement. Its basic cause is, as before, the asymmetry of the pressure distribution around the periphery of the ring.

Figure 13 illustrates the velocities and pressures. With a motionless concentric shaft, the flow is axi-symmetrical, and the velocity V_o is constant along the gap and around the periphery. Shaft displacement with the velocity V_s induces in the sealing gap squeeze film velocities, superimposed upon the steady flow velocity V_o. The continuity equation defines the maximum value of the induced velocity

$$V_x = V_s \frac{L}{2H}$$

The velocity along the gap is now not a constant V_o, but it varies in the closing gap from $(V_o - V_x)$ to $(V_o + V_x)$, and in the opening gap from $(V_o + V_x)$ to $(V_o - V_x)$.

This results both in a difference in the entry pressure losses, and in a distortion of the pressure gradient from a straight line to a parabola.

For $V_x << V_o$ the pressure variation can be described as follows: The difference in the entry pressure drop:

$$\Delta P_A = \frac{\rho}{2g}(1+\xi_1)\left[(V_o+V_x)^2-(V_o-V_x)^2\right]$$

$$\cong \frac{\rho}{2g}(1+\xi_1)\ 4\ V_o V_x$$

and the parabolic distortion of the pressure along the gap:

$$\Delta P_B = \frac{\rho}{2g} \cdot \frac{\lambda L}{4H}\left[V_o^2-\left(V_o-\frac{V_x}{2}\right)^2\right] \cong \frac{\rho}{2g}\frac{\lambda L}{4H} V_o\ V_x$$

The average pressure difference between the opening and the closing side becomes:

$$\Delta P = \frac{1}{2}\Delta P_A + \frac{4}{3}\Delta P_B + \frac{\rho}{2g}\left[2(1+\xi_1) + \frac{1}{3} \cdot \frac{\lambda L}{H}\right] V_o\ V_x \qquad (10)$$

V_x has been defined in (9) and V_o follows from

$$V_o = \sqrt{\frac{2g}{\rho}\ \frac{\Delta P}{(1+\xi_1)+\lambda L/2H}} \qquad (11)$$

Integration around the periphery gives the damping force as

$$F = \frac{\pi}{4} \cdot L \cdot D \cdot \Delta P \qquad (12)$$

Defining the damping coefficient as

$$C = \frac{F}{V_s} \qquad (13)$$

and combining equations (10) to (13) gives the value of the damping coefficient in smooth rings with pressure drop across to:

$$C = \frac{\pi}{4} \cdot \frac{DL^2}{H} \cdot \frac{(1+\xi_1+\lambda L/6H)}{\sqrt{1+\xi_1+\lambda L/2H}} \cdot \sqrt{\frac{\rho}{2g}\ \Delta P} \cdot \phi \qquad (14)$$

with the short circuit factor ϕ as defined in (7). Damping in grooved rings can be derived in a similar manner, and the pressure gradients are similar to Figure 13. The induced velocity is again

$$V_x = V_s\ \frac{L}{2H}$$

and the difference in the entry pressure drop is

$$\Delta P_A = \frac{\rho}{2g}\ (1+\xi_1)\ 4 \cdot V_o\ V_x$$

The camber of the parabolic pressure gradient can be approximated by

$$\Delta P_B = \frac{\rho}{2g}\ \xi_2\ \frac{n}{2}\left[\left(V_o+\frac{V_x}{2}\right)^2 - V_o^2\right] = \frac{\rho}{2g}\ \xi_2\ \frac{n}{2}\ V_o\ V_x$$

Using as typical values $\xi_1 = .5$, and $\xi_2 = .25$, the same transformation which led from (10) to (14) gives the damping coefficient in grooved rings with pressure drop to

$$C = \frac{\pi}{4} \cdot \frac{DL^2}{2H}\ (3 + .166\ n)\ \sqrt{\frac{\rho}{2g}\ \frac{\Delta P}{1.25 + .25\ n}}$$